

# The X-ray Spectrum and Light Curve of Supernova 1995N

D. W. Fox,<sup>1</sup> W. H. G. Lewin,<sup>1</sup> A. Fabian,<sup>2</sup> K. Iwasawa,<sup>2</sup> R. Terlevich,<sup>3</sup>  
 H. U. Zimmermann,<sup>4</sup> B. Aschenbach,<sup>4</sup> K. Weiler,<sup>5</sup> S. Van Dyk,<sup>6</sup> R. Chevalier,<sup>7</sup>  
 R. Rutledge,<sup>8</sup> H. Inoue,<sup>9</sup> S. Uno<sup>9</sup>

<sup>1</sup>MIT Center for Space Research, 77 Massachusetts Ave #37-627, Cambridge, MA 02139-4307, USA

<sup>2</sup>Institute of Astronomy, Madingley Road, Cambridge CB3 0HA

<sup>3</sup>Royal Greenwich Observatory, Madingley Road, Cambridge CB3 0EZ

<sup>4</sup>Max-Planck-Institut für Extraterrestrische Physik, Postfach 1312, D-85741 Garching, Germany

<sup>5</sup>Naval Research Laboratory, Washington, DC 20375-5300, USA

<sup>6</sup>IPAC/Caltech 100-22, Pasadena, CA 91115, USA

<sup>7</sup>Department of Astronomy, University of Virginia, Charlottesville, VA 22903-0818, USA

<sup>8</sup>California Institute of Technology MC 220-47, Pasadena, CA 91125, USA

<sup>9</sup>Institute of Space and Astronautical Science, Sagami-hara, Japan

Accepted date. Received date.

## ABSTRACT

We report on multi-epoch X-ray observations of the Type II<sub>n</sub> (narrow emission line) supernova SN 1995N with the *ROSAT* and *ASCA* satellites. The January 1998 *ASCA* X-ray spectrum is well fitted by a thermal bremsstrahlung ( $kT \sim 10$  keV,  $N_{\text{H}} \sim 6 \times 10^{20}$  cm<sup>-2</sup>) or power-law ( $\alpha \sim 1.7$ ,  $N_{\text{H}} \sim 10^{21}$  cm<sup>-2</sup>) model. The X-ray light curve shows evidence for significant flux evolution between August 1996 and January 1998: the count rate from the source decreased by 30% between our August 1996 and August 1997 *ROSAT* observations, and the X-ray luminosity most likely increased by a factor of  $\sim 2$  between our August 1997 *ROSAT* and January 1998 *ASCA* observations, although evolution of the spectral shape over this interval is not ruled out. The high X-ray luminosity,  $L_{\text{X}} \sim 10^{41}$  ergs s<sup>-1</sup>, places SN 1995N in a small group of Type II<sub>n</sub> supernovae with strong circumstellar interaction, and the evolving X-ray luminosity suggests that the circumstellar medium is distributed inhomogeneously.

**Key words:** supernovae: individual: SN 1995N – X-rays: stars – stars: circumstellar matter

## 1 INTRODUCTION

A small number of supernovae (SNe) have been detected in X-rays in the near aftermath ( $\sim$ years) of their explosions. SN 1978K, SN 1980K, SN 1986J, SN 1987A, and SN 1993J were found before 1995 (see Schlegel 1995 for a review); more recent detections include SN 1979C, SN 1988Z, and SN 1994I (Immler, Pietsch, & Aschenbach 1998a,b) and SN 1999em (Fox & Lewin 1999). Here we report on observations of SN 1995N (Pollas 1995).

Supernova X-ray emission depends on the density structure of the progenitor’s stellar wind as well as the structure of the SN ejecta, through which the initial shock passes. After the shock wave emerges from the star, the characteristic velocity is  $\sim 10^4$  km s<sup>-1</sup> and the density distribution in the outer parts of the star can be approximated by a power-law in radius,  $\rho \propto r^{-n}$ , where the value of  $n$  ranges from  $\sim 7$  to  $\sim 20$  (models for SN1987A have  $n \sim 10$ ; Matzner & McKee 1999). The shock then propagates into the circumstellar material, typically a slow-moving wind with a density that de-

creases with the inverse square of the radius,  $\rho = \dot{M}/4\pi r^2 v_w$ , where  $\dot{M}$  is the stellar wind mass-loss rate and  $v_w$  is the wind velocity (typically  $\sim 10$  km s<sup>-1</sup>). The collision between the stellar ejecta and the circumstellar material produces a second ‘reverse’ shock at  $\sim 1000$  km s<sup>-1</sup> in the stellar ejecta (which is expanding at  $\sim 10^4$  km s<sup>-1</sup>). The forward shock produces a very hot shell ( $\sim 10^9$  K), while the reverse shock produces a denser, cooler shell ( $\sim 10^7$  K) with much higher emission measure, from which the observable X-ray emission arises (Chevalier 1982). This picture is modified if the stellar wind is clumpy; then the forward shock front in the clumps can yield cooler, stronger emission than the shock front in the diffuse wind (Chugai 1993).

The exact time of the explosion of SN 1995N in the host galaxy MCG –02-38-017 is not known, but it may have occurred as much as ten months before its optical discovery in May 1995 (Benetti, Bouchet & Schwarz 1995), making the supernova  $\sim 2$  years old at the epoch of first detection (Lewin, Zimmermann, & Aschenbach 1996). SN 1995N was

**Table 1.** Log of SN 1995N X-ray observations

Date	Instrument	Exp. (sec)	Counts	Rate (ksec <sup>-1</sup> )
23 Jul 1996	<i>ROSAT</i> HRI	1311	9.4 ± 0.6	7.4 ± 3.5
12 Aug 1996	"	16991	163.6 ± 1.9	9.9 ± 0.9
17 Aug 1997	"	18797	126.4 ± 1.9	6.9 ± 0.7
20 Jan 1998	<i>ASCA</i> SIS	91129	1960.4 ± 29.6	29.7 ± 1.1
	<i>ASCA</i> GIS	95944	1300.7 ± 15.9	18.3 ± 0.8

Exposures are given in seconds, and count rates are in counts per kilosecond; *ASCA* ‘SIS’ and ‘GIS’ figures are for the SIS0+SIS1 and GIS2+GIS3 detector combinations, respectively (with the rates averaged between detectors). The quoted uncertainty in the number of counts detected is the uncertainty in the background subtraction only and does not take account of Poisson statistics. Count rates are corrected for the effects of the point spread function, and count rate uncertainties include the Poisson contribution.

only the fourth supernova to be detected in X-rays so soon after its explosion. Regular observations of the X-ray temperature, luminosity, and line-of-sight hydrogen column density will help determine the structure of the SN ejecta, the structure of the circumstellar medium established by the wind of the progenitor, and the details of its evolution prior to the explosion. These constraints can lead to an estimate of the progenitor stellar type and the type and length of its (pre-explosion) evolutionary stages.

## 2 OBSERVATIONS

We first observed SN 1995N in July 1996 with *ROSAT* when the optical (Benetti et al. 1995; Garnavich & Challis 1995) and radio (Van Dyk et al. 1996) properties of this supernova made it a promising candidate for strong X-ray emission. X-ray detection of SN 1995N with this pointing (Lewin et al. 1996) prompted our longer follow-up observation that August. In addition, we were awarded time for another *ROSAT* observation in August 1997, and applied simultaneously for *ASCA* spectral observations. Execution of our *ASCA* observation in January 1998 completed the program for this paper.

The log of our X-ray observations of SN 1995N is presented in Table 1. The standard photon screening criteria were adopted for all data sets (David et al. 1995; *ASCA* Data Reduction Guide<sup>\*</sup>). Source and background count rates were determined as follows.

*ROSAT* source counts were taken from a circle of radius 17.5 arcsec (35 pixels) centred on the SN position, and background counts were taken from an annulus of inner radius 20 arcsec and outer radius 50 arcsec. Source count rates (but not raw count numbers) were corrected for incompleteness due to the wings of the instrument point spread function (PSF), a 3% effect.

Two nearby X-ray sources complicated the process of choosing source and background extraction regions for the *ASCA* images. In Figure 1 we show the positions of SN 1995N and these X-ray sources, ‘A’ and ‘B’, overlaid on

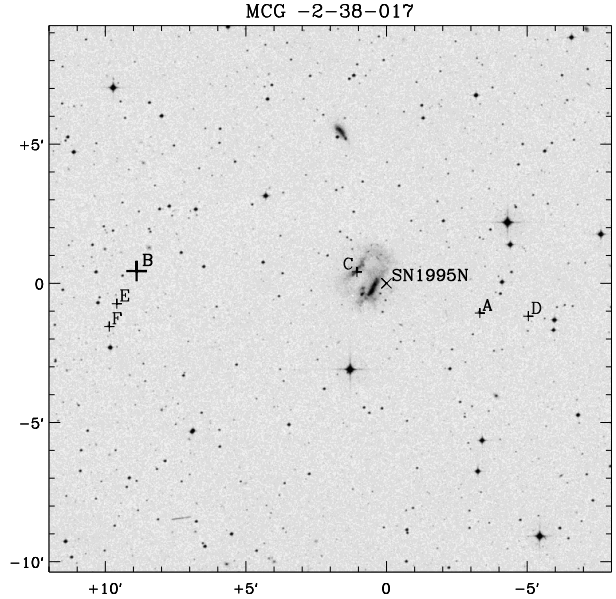


**Figure 1.** The SN 1995N field in the optical (*J* band, from the Digitized Sky Survey), showing the host galaxy MCG -02-38-017. Coordinates are in arcminutes relative to the position of SN 1995N, J2000 R.A. 14<sup>h</sup>49<sup>m</sup>28<sup>s</sup>.313, Dec -10°10'13".919 (indicated; Van Dyk et al. 1996). Positions of the nearby (*ASCA*) sources ‘A’ and ‘B’, and the additional (*ROSAT*) sources ‘C’–‘F’ are also shown. The *ASCA* GIS source ‘B’ is not detected in our *ROSAT* pointings, and therefore its positional uncertainty is substantial (~0.5 arcmin).

an optical image of the area from the Digitized Sky Survey. Also shown are four additional, weaker sources (‘C’–‘F’), visible in the summed HRI image, that are ignored in the *ASCA* analysis.

*ASCA* SIS source counts were taken from a circle of radius 4 arcmin (38 pixels) centred on the SN position, excluding a smaller circle (radius 15 pixels) around source A. Background counts were taken from the area of the CCD that remained after exclusion of the SN (38 pixel radius) and source A (24 pixel radius), and the SN count rate was corrected for the fraction of the PSF excluded (with the source area used expected to include 73% of the source counts).

*ASCA* GIS source counts were taken from a circle of radius 4.9 arcmin (20 pixels) centred on the SN position, excluding a smaller circle (radius 7 pixels) chosen on the basis of the SIS image to exclude counts from source A. Background counts were taken from a larger circle of radius 11.8 arcmin (48 pixels) centred on the SN, with circular areas removed to account for the SN (24 pixel radius), source A (18 pixel radius) and source B (20 pixel radius). The source area used here is expected to include 74% of the source counts.

## 3 ANALYSIS

### 3.1 Spectrum

Our X-ray spectral analysis made use only of the *ASCA* data, since the HRI does not have a spectral response sufficient for our purposes. After extracting source and background counts (see Sec. 2), we added the data from the

<sup>\*</sup> <http://heasarc.gsfc.nasa.gov/docs/asca/abc/abc.html>

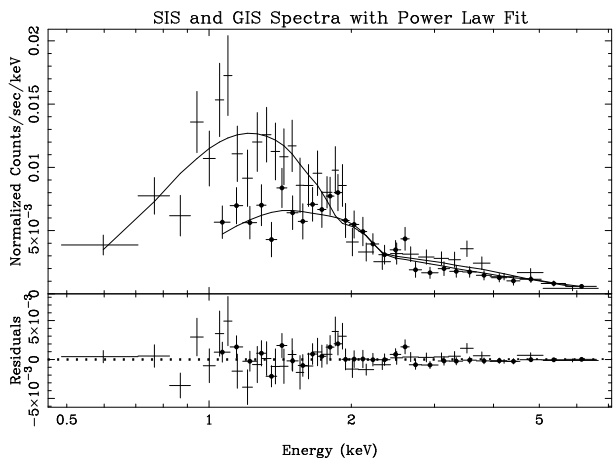


**Figure 2.** The X-ray spectrum of SN 1995N, with power-law model fit. The fitted power-law exponent (photon index) is  $\alpha = 1.7 \pm 0.1$  with an absorbing column  $N_{\text{H}} = 1.8 \pm 0.5 \times 10^{21} \text{ cm}^{-2}$ ; the spectrum may also be fit with a thermal bremsstrahlung model with  $kT = 9.1^{+2.7}_{-1.8} \text{ keV}$  (see Table 2). The residuals show a ‘bump’ near 1.8 keV, an appropriate energy for fluorescent Si emission, but the fit is not significantly improved by addition of an emission line at that energy.

two instrument pairs (SIS0+SIS1 and GIS2+GIS3) and produced averaged instrument response matrices for our analysis. We then ‘grouped’ spectral channels to achieve a minimum of  $\sim 20$  counts per channel above background.

X-ray spectral fitting was performed within the XSPEC environment (Arnaud 1996). We used the default modified Levenberg-Marquardt algorithm (derived from CURFIT, Bevington 1969) to minimize a  $\chi^2$  statistic that was calculated using the weighting scheme of Gehrels (1986); the statistical error on  $N$  counts was taken to be  $1 + \sqrt{N + 0.75}$ .

SIS (0.5–7.0 keV) and GIS (1.0–7.0 keV) spectra were fit simultaneously, with only the relative normalization of the model allowed to vary between the two datasets. This allowed for differential errors in our treatment of background subtraction and PSF effects between the two sets of instruments.

The quality of the spectrum (2000 SIS photons and 1300 GIS photons) does not make the examination of complex spectral models necessary or meaningful. On the contrary, as shown in Table 2, power-law and thermal bremsstrahlung spectra both provide acceptable fits to the data. MEKAL (Mewe, Gronenschild & van den Oord 1985) and Raymond-Smith plasma models also provide good fits to the data, but with the abundance parameter of these models essentially unconstrained in the fits, it is not clear what further conclusions the models allow us to draw. Plasma temperatures in the fits are  $kT = 6.9^{+1.4}_{-0.9} \text{ keV}$  (MEKAL) and  $kT = 8.8^{+2.9}_{-1.6} \text{ keV}$  (Raymond-Smith), with hydrogen column densities  $N_{\text{H}} \sim 10^{21} \text{ cm}^{-2}$ .

By contrast, a simple blackbody model (with absorption) was unable to fit the data and can be excluded – by comparison with the power law or bremsstrahlung models – with 99.9% confidence.

Figure 2 shows the observed X-ray spectrum with the power law fit superposed (the bremsstrahlung model fit does not differ visibly from this). Although there is a hint in the fit residuals of an additional feature near 1.8 keV, addition of

an absorption edge or spectrally unresolved emission line at this energy cannot be justified by the statistics (F-statistic confidence levels of 54% and 62%, respectively). Nevertheless, the energy is appropriate for fluorescent silicon emission (Si  $K\alpha$  and  $K\beta$  neutral line energies are 1.74 keV and 1.84 keV, respectively) and it is possible that the feature is real; if observations of other X-ray SNe with *Chandra* and *XMM-Newton* are able to detect a feature at this energy then the interpretation of our data will have to be revisited.

We note that the fitted hydrogen column densities under the two models are consistent with each other and with the Galactic column towards SN 1995N, which is  $7.8 \times 10^{20} \text{ cm}^{-2}$  (Dickey & Lockman 1990).

We examined the data near 6.7 keV for evidence of iron line emission and find none: our 90%-confidence upper limit for the equivalent width of a 6.7 keV iron line is 1.1 keV. Upper limits to the equivalent widths of lines centred at energies from 6.2 to 7.2 keV are all similarly  $\sim 1 \text{ keV}$ .

### 3.2 Light Curve

With an X-ray spectrum in hand we can proceed to calculate the incident flux and total X-ray luminosity of SN 1995N at the several epochs of our observations. These calculations are made under the assumption that (1) the spectrum of the source (apart from its overall normalization) was roughly constant over the timespan of the observations; and (2) that it is sufficiently well described by our models to allow extrapolations outside the energy range of our *ROSAT* and *ASCA* data. Note that in 1996 and 1997 we have only *ROSAT* data (no spectral information), and in 1998 we have only *ASCA* data (no sensitivity below 0.5 keV) – all other quoted fluxes and luminosities are based on model extrapolations.

Using the spectral fits as derived for the *ASCA* data of 1998 (see Sect. 3.1) and the PIMMS v3.0 software package<sup>†</sup>, we calculate the unabsorbed fluxes corresponding to the count rates observed in our *ROSAT* data, adding together the July and August 1996 pointings for better statistics; HRI count rates for the two observations are consistent with no change over the intervening 20 days (Table 1). Independently, we extrapolate our 1998 *ASCA* fluxes to the 0.1–2.4 keV range of the HRI for comparison purposes; the results are reported in Table 3. Since our power-law and thermal bremsstrahlung spectral models have different best-fit column densities, and this uncertainty dominates the Poisson uncertainty in our unabsorbed flux determinations, we report the flux conversions for the two models separately (in terms of a low and a high value) in Table 3. It should be noted, however, that in all likelihood the reported ranges still underestimate the actual uncertainty in unabsorbed source flux, since (1) the value of the best-fit hydrogen column for both models is relatively uncertain (Table 2); and (2) our spectral fits are subject to additional, unquantified, systematic uncertainties due to imperfect background subtraction. For example, if we reduce the hydrogen column to the Galactic value of  $7.8 \times 10^{20} \text{ cm}^{-2}$  – within the  $1\sigma$  range for our bremsstrahlung fit, and the  $2\sigma$  range for our power-law fit – then the fluxes calculated from our HRI observations are

<sup>†</sup> <http://heasarc.gsfc.nasa.gov/docs/software/tools/pimms.html>

**Table 2.** SN 1995N X-ray Spectral Fits

Model	$\chi^2_\nu$	$N_{\text{H}}$ ( $10^{21} \text{ cm}^{-2}$ )	Parameter	Flux (0.5–7 keV)	
				SIS	GIS
Power Law	0.956	$1.8 \pm 0.5$	$\alpha = 1.7 \pm 0.1$	$11.1 \pm 1.2$	$12.8 \pm 1.4$
Bremss.	0.999	$1.1 \pm 0.4$	$kT = 9.1^{+2.7}_{-1.8}$	$11.1 \pm 0.6$	$12.7 \pm 0.7$

Absorbed 0.5–7 keV flux is given in units of  $10^{-13} \text{ ergs cm}^{-2} \text{ s}^{-1}$ , and is corrected for incompleteness due to the instrument point spread functions. The power-law index  $\alpha$  is the photon spectral index. Reduced chi-squared values are calculated using a Gehrels weighting (Gehrels 1986). Note that the Galactic neutral hydrogen column in the direction of SN 1995N is  $7.8 \times 10^{20} \text{ cm}^{-2}$  (Dickey & Lockman 1990).

**Table 3.** X-ray flux history of SN 1995N

Date	Instr.	Unabsorbed Flux		$L_X$	Stat. Unc.
		0.1–2.4 keV	0.5–7.0 keV		
Jul–Aug 1996	HRI	6.3–8.9	9.9–11.0	12	9
17 Aug 1997	HRI	4.5–6.3	7.0–7.8	8	10
20 Jan 1998	SIS	7.5–10.5	12.2–13.2	14	5
	GIS	8.6–11.5	14.0–15.2	15	5

Unabsorbed fluxes are in units of  $10^{-13} \text{ ergs cm}^{-2} \text{ s}^{-1}$ , within the energy ranges indicated. Luminosities  $L_X$  (0.1–10 keV; assumed isotropic) are in units of  $10^{40} \text{ ergs s}^{-1}$ , and are calculated using the Galactic hydrogen column  $N_{\text{H}} = 7.8 \times 10^{20} \text{ cm}^{-2}$  and a distance of 28 Mpc. Flux ranges indicate the variation in photon-to-flux conversion for our two best-fit spectral models, thermal bremsstrahlung (left) and power-law (right), due mainly to the difference in the fitted hydrogen column (see Sec. 3.1). The additional percentage error introduced by the statistical uncertainty in the number of photons detected for each observation is shown. Since the hydrogen column measurement has additional statistical and systematic uncertainties, these ranges are likely to be overoptimistic (see text for details).

reduced by a further 10% relative to the lower end of the ranges given in Table 3.

Accepting these caveats, we may draw the following conclusions. First, the *ROSAT* observations indicate (at >4-sigma confidence) a 30% decrease in absorbed 0.1–2.4 keV X-ray flux between August 1996 and August 1997 (Table 1). Second, comparison of the August 1997 *ROSAT* observation with the January 1998 *ASCA* observation (Table 3) indicates that the X-ray luminosity of SN 1995N may have increased by a factor of  $\approx 2$  over this time. Alternatively, the spectrum may have changed significantly (contrary to our Assumption 1 above); however, to make the August 1997 observation consistent with  $L_X = 1.5 \times 10^{41} \text{ ergs s}^{-1}$  requires either absorption of  $N_{\text{H}} \sim 4 \times 10^{21} \text{ cm}^{-2}$  or an unlikely (temporary) hardening of the spectrum to  $kT > 50 \text{ keV}$  or  $\alpha < 1.02$ . Thus, the conclusion that the SN dimmed from August 1996 to August 1997 and then brightened from August 1997 to January 1998 seems the most probable explanation for our data.

## 4 DISCUSSION

The optical spectra of SN 1995N show that it belongs to the Type IIn (narrow line) category (Benetti et al. 1995). A

number of other Type IIn supernovae have been detected as strong X-ray sources and their properties are summarized in Table 4. These supernovae are the most luminous X-ray supernovae and are inferred to be interacting with a dense circumstellar medium. They are also luminous radio supernovae. The X-ray luminosity of SN 1995N places it in this highly luminous group.

The interpretation of the X-ray emission from these sources is not clear. Chevalier & Fransson (1994) presented models in which smooth supernova ejecta interact with a smooth circumstellar wind. In this picture, the reverse shock emission is characterized by  $kT \approx 1 \text{ keV}$  and the forward shock emission by  $kT \approx 100 \text{ keV}$ . However, the radio emission (see Weiler et al. 1990 for SN 1986J) and narrow optical line emission give evidence that the circumstellar medium is clumpy and shock waves are being driven into the clumps (see Chugai et al. 1995 on the case of SN 1978K). Supernovae like SN 1978K and SN 1988Z show very narrow line emission, which can be attributed to dense circumstellar clumps that are photo-ionized by the X-ray emission, and line components with a width of  $\sim 2,000 \text{ km s}^{-1}$  that can be from cooling shocks moving into the clumps. SN 1995N also shows evidence for these line components (A.V. Filippenko, priv. comm.). Shock waves in clumps can give cooler X-ray emission than the forward shock front in the diffuse circumstellar medium. Chugai (1993) found that this picture may be preferred for the X-ray emission from SN 1986J. A prediction of this model is that the emitting region should have a lower characteristic velocity than in the case of the reverse shock wave.

Our series of flux measurements show that the X-ray luminosity of SN 1995N has probably dimmed by 30% and then brightened by as much as a factor of two over the period of observation, which corresponds to an age range of 2.0 to 3.5 years for a proposed explosion date in July 1994 (Benetti et al. 1995). The X-ray light curve of SN 1978K shows approximately constant luminosity over the age range of 12 to 16 years (Schlegel, Petre, & Colbert 1996). For SN 1986J, a decline in luminosity has been observed over the age range 8.6 to 13 years (Houck et al. 1998); the evolution is consistent with a  $t^{-2}$  time dependence. In the models of Chevalier & Fransson (1994), a decline in flux is expected if the evolution is non-radiative, whereas a radiative reverse shock front leads to a roughly constant luminosity. In the clump model (Chugai 1993), the evolution depends on the variation of clump properties with radius. The light curve that we observe may be due to such variation.

**Table 4.** Type IIn X-ray Supernovae

Supernova	Distance (Mpc)	$\log L_X$ (ergs s <sup>-1</sup> )	$kT$ (keV)	$\log N_H$ (cm <sup>-2</sup> )	Refs.
SN 1978K	4.5	40.3	3	≈20	(1),(2)
SN 1986J	10	40.3	5.0–7.5	21.7	(3)
SN 1988Z	98	41.0			(4)
SN 1995N	28	41.2	9	20.9	(5)

$L_X$  is the peak observed X-ray luminosity (0.1–10 keV). References are: (1) Petre et al. 1994; (2) Schlegel et al. 1996; (3) Houck et al. 1998; (4) Fabian & Terlevich 1996; (5) this paper.

Characterization of the radio observations of SN 1995N is not yet complete. However, five 8.4 GHz radio observations made between July 1995 and June 1998 are all consistent with a constant flux of 3.8 mJy (Van Dyk et al. 2000), indicating only mild evolution of the radio properties of the shocked region over this interval.

In Table 4, we give the estimated temperature characterizing the X-ray emission, although it is only in the case of SN 1986J that an X-ray line has been detected (Houck et al. 1998), and hence, the presence of thermal emission confirmed. Possible non-thermal sources of X-ray emission are inverse Compton and synchrotron emission, but these are typically less efficient than thermal emission (Chevalier 1982). The temperature that we find is higher than expected for the reverse shock wave, but somewhat lower than that expected for the forward shock wave. If the emission is from shocked clumps, the temperature depends on the density of the clumps, so that intermediate temperatures are possible. The lack of detectable line emission does not allow us to directly test for the presence of clumps by examining the widths of lines.

The gas column density that we measure to the source is compatible (within our roughly 50% uncertainty) with the expected column density in our Galaxy. Table 4 shows that a higher column density is present to SN 1986J, but that can be attributed to absorption within the parent galaxy (Houck et al. 1998). These supernovae do not show evidence for absorption by the dense shell that might be formed by a cooling reverse shock wave. Since the cool shell formed by a reverse shock will probably not be ionized, two years or more after the SN explosion, this low absorption may indicate inhomogeneities in the shell that allow the X-ray flux to emerge without absorption. Alternatively, low absorption may be seen as supporting the clump model (Chugai 1993), since the X-ray emission from forward shocks penetrating high-density clumps will not be significantly absorbed.

## 5 CONCLUSIONS

Our observations show that SN 1995N belongs to the class of X-ray luminous Type IIn supernovae. The variations in X-ray flux over a 1.5 yr period suggest that the emission mechanism is more complicated than simple radiative emission from a reverse shock wave generated by interaction with a dense circumstellar medium, and that inhomogeneities in the circumstellar medium play a role. The X-ray emission is expected to power the optical/ultraviolet emission from the

supernova; thus, optical spectroscopy will provide information on the gas motions so that a model for the supernova and the circumstellar structure can be determined.

## 5.1 Acknowledgments

WHGL and RC gratefully acknowledge support from the National Aeronautics and Space Administration. KWW thanks the office of Naval Research for the 6.1 support of this research. This research has made use of the Digitized Sky Survey, produced at the Space Telescope Science Institute under U.S. Government grant NAG W-2166.

## REFERENCES

- Arnaud K., 1996, *Astronomical Data Analysis Software and Systems V*, Eds. Jacoby G., Branes J., p. 17, ASP Conf. Series Vol. 101
- Benetti S., Bouchet P., Schwarz H., 1995, IAUC 6170
- Bevington R., 1969, *Data Reduction and Error Analysis for the Physical Sciences*, McGraw-Hill, New York
- Chevalier R.A., 1982, ApJ, 259, 302
- Chevalier R.A., Fransson C., 1994, ApJ, 420, 268
- Chugai N.N., 1993, ApJ, 414, L101
- Chugai N.N., Danziger, I. J., Della Valle, M., 1995, MNRAS, 276, 530
- David L. P., Harnden Jr. F. R., Kearns K. E., Zombeck M. V., 1995, *The ROSAT High Resolution Imager*. U.S. ROSAT Science Data Center/SAO, Cambridge, MA
- Dickey J.M., Lockman F.J., 1990, ARAA, 28, 215
- Fabian A.C., Terlevich R., 1996, MNRAS, 280, L5
- Fox D.W., Lewin W.H.G., 1999, IAUC 7318
- Garnavich P., Challis P., 1995, IAUC 6174
- Gehrels N., 1986, ApJ, 303, 336
- Houck J.C., Bregman J.N., Chevalier R.A., Tomisaka K., 1998, ApJ, 493, 431
- Immler, S., Pietsch, W., Aschenbach, B. 1998a, A&A, 331, 601
- Immler, S., Pietsch, W., Aschenbach, B. 1998b, A&A, 336, L1
- Lewin W., Zimmermann H.U., Aschenbach B., 1996, IAUC 6445
- Matzner, C.D., McKee C.F., 1999, ApJ, 510, 379
- Mewe R., Gronenschild E.H.B.M., van den Oord G.H.J., 1985, A&AS, 62, 197
- Petre R., Okada, K., Mihara, T. Makishima, K, Colbert, E. J. M., 1994, PASJ, 46, L115
- Pollas C., 1995, IAUC 6170
- Schlegel, E. M. 1995, Rep. Prog. Phys. 58, 1375
- Schlegel, E. M., Petre, R., Colbert, E. J. M. 1996, ApJ, 456, 187
- Van Dyk S.D., Sramek R.A., Weiler K.W., Montes M.J., Panagia N., 1996, IAUC 6386
- Van Dyk S.D., et al., 2000, in preparation

Weiler K.W., Panagia N., Sramek R.A., 1990, ApJ, 364, 611